Paper from: *Advanced Computational Methods in Heat Transfer*, B Sunden and CA Brebbia (Editors).
ISBN 1-85312-906-2

Modeling heat transfer using adaptive finite elements, boundary elements, and meshless methods

D.W. Pepper[1], C.S. Chen[2] & J. Li[2]
[1]*Department of Mechanical Engineering, University of Nevada Las Vegas, USA*
[2]*Department of Mathematics, University of Nevada Las Vegas, USA*

Abstract

While many numerical schemes exist for solving heat transfer problems, several numerical techniques have become particularly attractive and of interest to the modeling community. Finite element methods that use some form of adaptation (h- and/or p-adaptation), boundary elements, and meshless methods are three schemes that are especially promising. In this study, solutions obtained using a finite element scheme that employs h-adaptation are compared with boundary element and meshless methods for several heat transfer test problems. Each method has its merits and deficiencies. Additional information can be found on the web site http://www.unlv.edu/Research_Centers/NCACM.

1 Introduction

For the engineer interested in thermal analysis, the ability to accurately simulate heat transfer processes in all types of geometry is important. Finite difference (FDM), finite volume (FVM), and finite element methods (FEM) have been used for many years to model such problems. Early numerical models followed conventional approaches that required large storage demands and long computing times. Today, improvements in these numerical schemes and

---

[1] Professor and Chairman, Department of Mechanical Engineering; Director, Nevada Center for Adv. Comput. Meth. (NCACM)
[2] Professor, Department of Mathematics
[3] Assistant Professor, Department of Mathematics

Paper from: *Advanced Computational Methods in Heat Transfer*, B Sunden and CA Brebbia (Editors).
ISBN 1-85312-906-2

enhanced hardware have lead to many commercial codes that have become recognized standards for simulating heat transfer in academia and industry [1,2]. More recently, advances in the application of h-adaptive FEM, boundary element methods (BEM), and meshless methods (MLM) have clearly shown that they are strong competitors to these more classical numerical approaches and should be considered as viable alternatives. In this study, solutions using h-adaptive finite elements, boundary elements, and meshless methods are obtained and a comparison of results discussed for several heat transfer examples.

2 Governing Equations

The governing equation consists of the terms that describe the advection and diffusion of heat, commonly written as

$$\frac{\partial T}{\partial t} + \mathbf{V} \cdot \nabla T = \alpha \nabla^2 T + Q \tag{1}$$

$$q + k\nabla T - h(T - T_\infty) - \varepsilon\sigma(T^4 - T_\infty^4) = 0 \tag{2}$$

$$T(\mathbf{x}, 0) = T_o \tag{3}$$

where $\mathbf{V}$ is the vector velocity, $\mathbf{x}$ is vector space, $T(\mathbf{x},t)$ is temperature, T_∞ is ambient temperature, T_o is initial temperature, α is thermal diffusivity ($\kappa/\rho c_p$), ε is emissivity, σ is the Stefan-Boltzmann constant, h is the convective film coefficient, q is heat flux, and Q is heat source/sink.

3 Finite Element Method (FEM)

The standard weak formulation of the Galerkin weighted residual technique is employed to cast the energy equation into integral form:

$$\int_\Omega W \cdot [\frac{\partial T}{\partial t} + (\mathbf{V} \cdot \nabla)T + \alpha \nabla W : \nabla T - Q] d\Omega - \int_\Gamma \alpha W \cdot (\mathbf{n} \cdot \nabla T) d\Gamma = 0 \tag{4}$$

where $\nabla W : \nabla T \equiv [\partial W/\partial x_j][\partial T_i/\partial x_j]^T$, W is the weighting function, Ω is the computational domain with boundary Γ, and $\mathbf{n}$ is the unit vector normal to Γ. The boundary integral, which arises from the application of Green's identity on the diffusion term, provides a natural mechanism for implementing flux boundary conditions. The temperature is replaced by the trial approximation

$$T(\mathbf{x}, t) = \sum_{i=1}^{n} N_i(\mathbf{x}) T_i(t) \tag{5}$$

Paper from: *Advanced Computational Methods in Heat Transfer*, B Sunden and CA Brebbia (Editors).
ISBN 1-85312-906-2

where N_i is the bilinear basis function and n is the number of local nodes per element. Typically triangular (3-noded) or quadrilateral isoparametric (4-noded) elements are used to discretize 2-D problem domains, such as shown in Fig. 1.

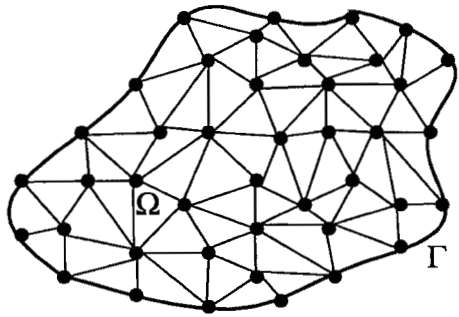

Figure 1. Irregular domain discretized using 3-noded triangular elements.

Equation (4) can be written in matrix form by setting $W = N_i$. Note that the weighting function in the advection matrix is not set equal to N_i, but rather to a Petrov-Galerkin weighting scheme [3,4]. The resulting matrix equation for temperature is

$$[M]\{\dot{T}\}+[K_T]\{T\}+[A(\mathbf{V})]\{T\}=\{F_T\} \tag{6}$$

where [ ] denotes an n x n sparse matrix, { } is the column vector of n unknowns, and the . refers to time differentiation of the nodal quantities. Gaussian quadrature is used in the numerical evaluation of these equations. However, in regions where elements are uniform, reduced integration is used to enhance solution speed.

Mass lumping is employed to permit explicit time integration without the need for total matrix inversion. This is achieved by summing the consistent mass matrix row values into single diagonal values. Temperature is subsequently solved using an explicit Euler scheme,

$$\{T\}^{n+1}=\{T\}^{n}+\Delta t\left[M^{l}\right]^{-1}\left[\{F_T\}-([K_T]+[A(\mathbf{V})])\{T\}^{n}-Q\right] \tag{7}$$

where superscript n indicates quantities evaluated at time $n\Delta t$, with Δt being the time step. To maintain stability, both Courant and diffusive limits are calculated over each element, and the time step adjusted to permit global stability.

Velocities are assumed to be known; u and v values are typically obtained from solution of the equations of motion (a separate adaptive program is used for fluid flow and convective heat transfer [5]), or solution of Laplace's equation to obtain a potential flow field from which u and v components can be extracted. This option requires the user to specify boundary conditions for the potential.

Paper from: *Advanced Computational Methods in Heat Transfer*, B Sunden and CA Brebbia (Editors).
ISBN 1-85312-906-2

3.1 h-adaptation

In h-adaptation, the computational mesh refines and unrefines by adding and subtracting elements within the computational domain as the solution evolves in time. The number of elements (and node points) are increased in regions of high gradients, and reduced where the flow is smooth.

Elements that need to be refined or unrefined are identified; refinement proceeds from the coarsest level to the finest level. The adaptive refinement threshold values are generally determined empirically; these values can be varied to cause more or less elements to be refined or unrefined, depending upon desired accuracy and computer time. After all the mesh changes have been made, the grid geometry is recalculated; the solution is interpolated onto the new grid, and the calculation procedure begun again. For steady state situations, the entire procedure is repeated until a *converged* mesh is obtained (several times is usually sufficient). More detailed descriptions of adaptation techniques are discussed in Huang and Usmani [2] and Pepper and Stephenson [3].

Local mesh refinement (h-adaptation), when used with a Petrov-Galerkin finite element technique, can yield very accurate solutions to a wide range of advection-diffusion problems [5,6]. When one elects to use p-adaptation (refining the shape functions) either alone or with h-adaptation, an especially high order numerical scheme evolves that can achieve exponential convergence. While each method has its own particular strengths and weaknesses, the combined strength of both techniques leads to a very powerful method that can be used for a wide variety of nonlinear transport-related problems.

4 The Boundary Element Method (BEM)

The boundary element method (BEM) is a unique numerical scheme that permits rapid and accurate solution of a specific class of equations [7,8]. Employing Green's identity, the boundary element method requires only the discretization of the boundary domain - no internal mesh is required as in the finite element method.

One begins by applying the weighted residual technique to the governing equation (Eq. 1) using a weighting function T* which is the fundamental solution of the steady-state temperature equation [8], i.e.,

$$\int_{\Omega}\left(\alpha\nabla^2 T - V\cdot\nabla T\right)T^* d\Omega = \int_{\Omega}\frac{\partial T}{\partial t}T^* d\Omega \qquad (8)$$

Integrating the Laplacian by parts twice and the first order space derivatives once yields

$$T(\xi) - \alpha\int_{\Gamma}T^*\frac{\partial T}{\partial n}d\Gamma + \alpha\int_{\Gamma}T\frac{\partial T^*}{\partial n}d\Gamma + \int_{\Gamma}TT^*V_n d\Gamma = \int_{\Omega}\frac{\partial T}{\partial n}T^* d\Omega \qquad (9)$$

where V_n is the velocity normal to a boundary and ∂n denotes the normal boundary gradient. The corresponding boundary integral equation, for source point ξ on the boundary, becomes

Paper from: *Advanced Computational Methods in Heat Transfer*, B Sunden and CA Brebbia (Editors).
ISBN 1-85312-906-2

$$c(\xi)T(\xi)-\alpha\int_{\Gamma}T^{*}\frac{\partial T}{\partial n}d\Gamma+\alpha\int_{\Gamma}T\frac{\partial T^{*}}{\partial n}d\Gamma+\int_{\Gamma}TT^{*}V_{n}d\Gamma=\int_{\Omega}\frac{\partial T}{\partial n}T^{*}d\Omega \quad (10)$$

with $c(\xi)$ a function of the internal angle the boundary Γ makes at point ξ. In order to obtain a boundary integral equivalent to the domain integral, a dual reciprocity approximation is introduced [8]. The time derivative term is expanded into the form

$$\int_{\Omega}\frac{\partial T}{\partial t}T^{*}d\Omega=\sum_{k=1}^{P}\lambda_{k}(t)\int_{\Omega}f_{k}(\mathbf{x})T^{*}d\Omega \quad (11)$$

where f_k are known functions dependent only on geometry and λ_k is dependent only on time. For each function f_k there exists a related function ψ_k that is a particular solution of the steady-state form of Eq. (1). The domain integral can be recast into the form

$$\int_{\Omega}\frac{\partial T}{\partial t}T^{*}d\Omega=\sum_{k=1}^{P}\lambda_{k}(t)\int_{\Omega}\left(\alpha\nabla^{2}\psi_{k}-V\cdot\nabla\psi_{k}\right)T^{*}d\Omega \quad (12)$$

Substituting Eq. (12) into Eq. (11) and applying integration by parts to the RHS of the resulting equation, the boundary integral equation becomes

$$\begin{aligned}&c_{i}T_{i}-\sum_{j=1}^{N}\alpha\int_{\Gamma}T^{*}\frac{\partial T}{\partial n}d\Gamma+\sum_{j=1}^{N}\alpha\int_{\Gamma}\left(\frac{\partial T^{*}}{\partial n}+\frac{V_{n}}{K}T^{*}\right)TdT=\\&\sum_{k=1}^{P}\lambda_{k}\left[c_{i}\psi_{ik}-\sum_{j=1}^{N}\alpha\int_{\Gamma}T^{*}\frac{\partial\psi_{k}}{\partial n}d\Gamma+\sum_{j=1}^{N}\alpha\int_{\Gamma}\left(\frac{\partial T^{*}}{\partial n}+\frac{V_{n}}{K}T^{*}\right)\psi_{k}d\Gamma\right]\end{aligned} \quad (13)$$

The variation of T, $q = \partial T/\partial n$, ψ and $\eta = \partial\psi/\partial n$ within each boundary element is approximated by interpolating from values at the element nodes. Hence, the following matrix equivalent form of Eq. (13) is

$$[H]\{T\}-[G]\{q\}=([H][\psi]-[G][\eta])\{\lambda\} \quad (14)$$

where [H], [G], $[\psi]$, and $[\eta]$ are banded geometry-dependent matrices and T, q, and λ are nodal vectors. Employing a two-level time integration scheme, the discrete form of the final matrix equation becomes

$$\begin{aligned}&\left(\frac{1}{\Delta t}[C]+\theta[H]\right)\{T\}^{n+1}-\theta[G]\{q\}^{n+1}=\\&\left(\frac{1}{\Delta t}[C]-(1-\theta)[H]\right)\{T\}^{n}+(1-\theta)\{q\}^{n}\end{aligned} \quad (15)$$

where $\frac{1}{2}\le\theta\le 1$ and

$$[C]=-([H][\psi]-[G][\eta])F^{-1},\quad \text{and } \{\lambda\}=[F]^{-1}\left\{\frac{\partial T}{\partial t}\right\} \quad (16)$$

There is no need to establish an interior nodal mesh common to FDM, FVM, and FEM. Figure 2 shows an irregular domain with boundary nodes; interior

Paper from: *Advanced Computational Methods in Heat Transfer*, B Sunden and CA Brebbia (Editors).
ISBN 1-85312-906-2

nodes are specified where desired by the user.

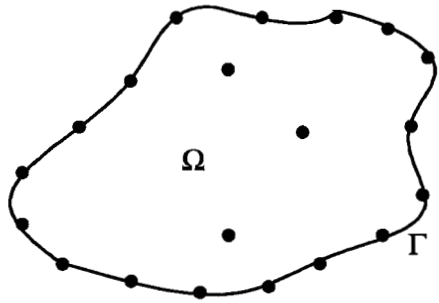

Figure 2. Boundary element method showing boundary and interior nodes

5 Meshless Methods (MLM)

Meshless methods are uniquely simple, yet provide solution accuracies for certain classes of equations that rival those of finite elements and boundary elements without requiring the need for mesh connectivity. Ease in programming, no domain or surface discretization, no numerical integration, and similar formulations for 2-D and 3-D make these methods very attractive.

There exist several types of meshless methods, such as kernel methods, moving least square method, partition of unity methods, and radial basis functions. Additional references on meshless methods can be found in [9]. The meshless method (MLM) examined in this study is based on the use of radial basis functions and Kansa's approach [10].

In Kansa's method, the temperature is approximated using the expression

$$T(\mathbf{x}) = \sum_{j=1}^{N} \phi(\mathbf{x}) T_j \tag{17}$$

where $\{T_j\}$ are the unknown coefficients and $\phi_j(x) = \phi\|x\text{-}x_j\|$ is some form of radial basis function where $\{x_i\}_1^{N_I}$ are interior points and $\{x_i\}_{N_I+1}^{N}$ are boundary points. Some commonly used radial basis functions (RBFs) include

Linear: r

Cubic: r^3

Multiquadrics (MQ): $\sqrt{r^2 + c^2}$ where c is a shape parameter (18)

Polyharmonic Splines: $\begin{cases} r^{2n} \log r, \; n \geq 1 \text{ in 2-D} \\ r^{2n-1}, \; n \geq 1 \text{ in 3-D} \end{cases}$

Gaussian: e^{-cr^2}

The theory of RBFs interpolation is discussed in Powell [11].

Paper from: *Advanced Computational Methods in Heat Transfer*, B Sunden and CA Brebbia (Editors).
ISBN 1-85312-906-2

To illustrate the application of the MLM with RBF, consider the simple Poisson's equation

$$\begin{aligned} \nabla^2 T &= f(\mathbf{x}) \quad (\mathbf{x}) \in \Omega \\ T &= g(\mathbf{x}) \quad (\mathbf{x}) \in \Gamma \end{aligned} \tag{19}$$

Now approximate T assuming

$$T(\mathbf{x}) = \sum_{j=1}^{N} \phi(r_j) T_j \tag{20}$$

where r is defined as

$$r_j = \sqrt{(x - x_j)^2 + (y - y_j)^2} \tag{21}$$

Using multiquadrics as a basis function, one obtains

$$\phi(r_j) = \sqrt{r_j^2 + c^2} = \sqrt{(x - x_j)^2 + (y - y_j)^2 + c^2} \tag{22}$$

Likewise, the derivatives can be expressed as

$$\begin{aligned} \frac{\partial \phi}{\partial x} &= \frac{x - x_j}{\sqrt{r_j^2 + c^2}}, \quad \frac{\partial \phi}{\partial y} = \frac{y - y_j}{\sqrt{r_j^2 + c^2}} \\ \frac{\partial^2 \phi}{\partial x^2} &= \frac{(y - y_j)^2 + c^2}{\sqrt{r_j^2 + c^2}}, \quad \frac{\partial^2 \phi}{\partial y^2} = \frac{(x - x_j)^2 + c^2}{\sqrt{r_j^2 + c^2}} \end{aligned} \tag{23}$$

Substituting into the original equation set, one obtains

$$\begin{aligned} \sum_{j=1}^{N} \nabla^2 \phi(r_j) T_j &= f(\mathbf{x}), \quad i = 1, 2, \cdots, N_I \\ \sum_{j=1}^{N} \phi(r_j) T_j &= g(\mathbf{x}), \quad i = N_I + 1, N_I + 2, \cdots, N \end{aligned} \tag{24}$$

This is illustrated in Fig. 3 showing the arbitrarily distributed interior and boundary points.

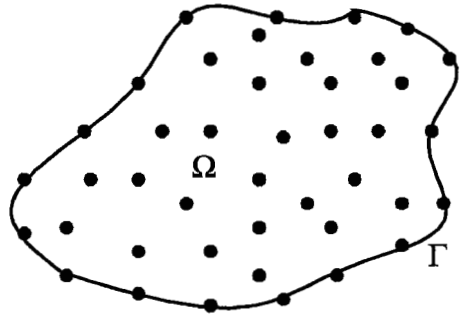

Figure 3. Interior and boundary points for the meshless method

For the 2-D transport equation for heat transfer, the relation becomes

Paper from: *Advanced Computational Methods in Heat Transfer*, B Sunden and CA Brebbia (Editors).
ISBN 1-85312-906-2

$$\sum_{j=1}^{N}\left(\frac{\phi(r_j)}{\Delta t}-\alpha\nabla^2\phi(r_j)\right)T_j^n=\frac{T^n(r_i)}{\Delta t}-V\cdot\nabla T(r_i),\quad i=1,2,\cdots,N_I$$
$$\sum_{j=1}^{N}\phi(r_j)T_j^n=g(x,t),\quad i=N_I+1,N_I+2,\cdots,N \tag{25}$$

from which one can solve the N X N linear system for the unknown temperature $\{T_j\}$ and obtain the approximate solution at any point in the domain, Ω.

6 Example Problems

6.1 Comparison with exact solution in a rectangular domain

In this first problem, a two-dimensional plate is subjected to prescribed temperatures applied along each boundary [12], as shown in Fig. 4. The temperature at the mid-point (1,0.5) is used to compare the numerical solutions with the analytical solution. The analytical solution is T(1,0.5) = 94.5°C [12].

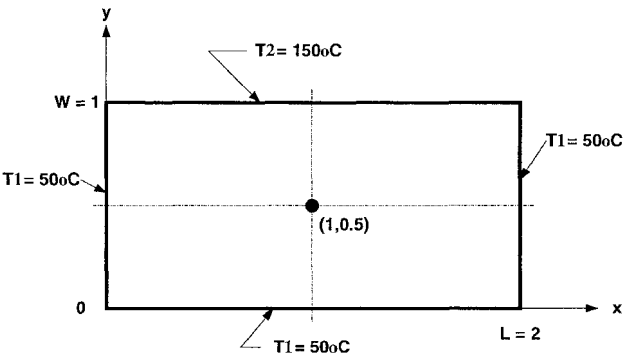

Figure 4: Steady-state conduction in a two-dimensional plate (from [12]).

Figure 5 shows the final computational mesh (starting with an initial 10 x 10 mesh) and resulting temperature contours obtained from the FEM model. Table 1 lists the final temperatures at the mid-point for the three numerical methods. The same boundary and internal nodes were used in the BEM; linear 2-noded elements were used to discretize the boundaries for the BEM.

Table 1. Comparison of results for problem 1 from Exact, FEM, BEM, and MFS

Method	mid-point (°C)	Elements	Nodes
Exact	94.512	0	0
FEM	94.605	256	289
BEM	94.471	64	65
MLM	94.514	0	325

Paper from: *Advanced Computational Methods in Heat Transfer*, B Sunden and CA Brebbia (Editors).
ISBN 1-85312-906-2

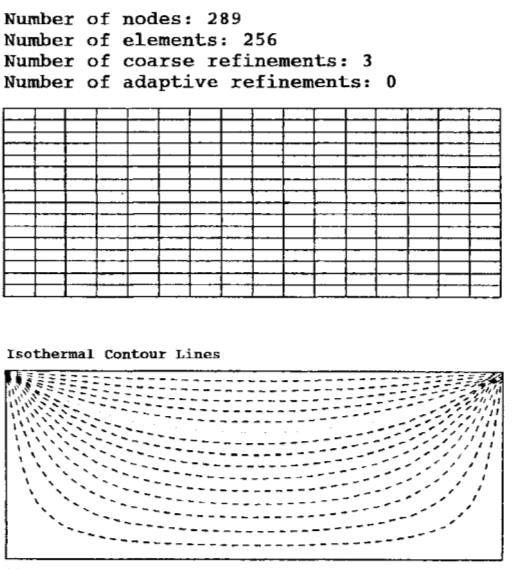

Figure 5: FEM computational mesh and isotherms for two-dimensional plate.

6.2 Heat transfer with convection in a rectangular domain

In the second problem, a two-dimensional domain is prescribed with Dirichlet and Neumann boundary conditions applied along the boundaries, as shown in Fig. 6. This problem, described in Huang and Usmani [2], was used to assess an h-adaptive FEM technique for accuracy. A fixed temperature of 100°C is set along side AB; a surface convection of 0°C acts along edge BC and DC with h = 750 W/m°C and k = 52 W/m°C. The temperature at point E is used for comparative purposes. The severe discontinuity in boundary conditions at point B creates a steep temperature gradient between points B and E. Figure 7 shows the final FEM meshes after two adaptations using bilinear triangular and quadrilateral elements [2]. The analytical solution for the temperature at point B is T = 18.2535°C. Table 2 lists the results for the three methods compared with the exact solution. The initial number of elements and nodes for the 3-noded triangular mesh was 25 elements and 19 nodes; for the 4-node quadrilateral, the initial values were 8 elements and 15 nodes. As expected, the FEM mesh refined near points B and E, and unrefined in areas furthest from the discontinuity.

Table 2. Comparison of results for problem 2 from Exact, FEM, BEM, and MFS

Method	Point E (°C)	Elements (3/4)	Nodes (3/4)
Exact	18.2535	0	0
FEM	18.1141	256/89	155/105
BEM	18.2335	32	32
MLM	18.2531	0	83

Paper from: *Advanced Computational Methods in Heat Transfer*, B Sunden and CA Brebbia (Editors).
ISBN 1-85312-906-2

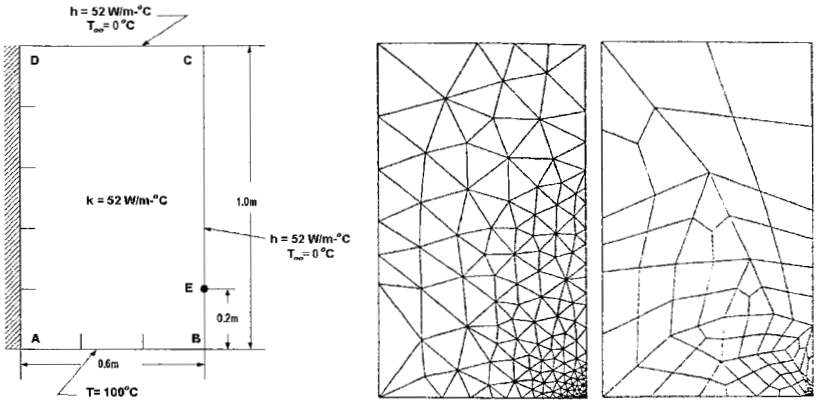

(a) (b)

Figure 6. Problem 2 (a) domain and (b) final FEM meshes (from [2]).

6.3 Heat transfer in an irregular domain

A simple irregular domain is used for the last example problem and results compared from the three methods. Results from a fine mesh FEM solution (without adaptation) are used as a reference benchmark [6]. The discretized domain and accompanying boundary conditions set along each surface are shown in Fig. 7. FEM results are displayed as contour intervals. Figure 8(a,b) shows FEM solutions for fine and adapted meshes. Exactly where adaptive meshing occurs is not initially evident. As can be seen in Fig. 8(b), three of the corners produce finer meshing as a result of steep temperature gradients; this is not evident when using BEM or MLM methods.

The BEM and MLM mid-point values at (0.5,0.5) are listed in Table 3 along with the FEM results. The BEM used the same number of boundary nodes and locations as used in the initial FEM mesh (Fig. 7); the MLM used 46 meshless points for the boundary and 50 interior nodes.

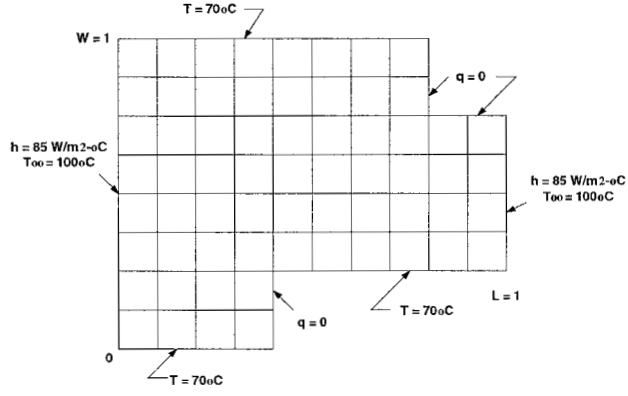

Figure 7: Problem specification for heat transfer in a user-defined domain.

Paper from: *Advanced Computational Methods in Heat Transfer*, B Sunden and CA Brebbia (Editors).
ISBN 1-85312-906-2

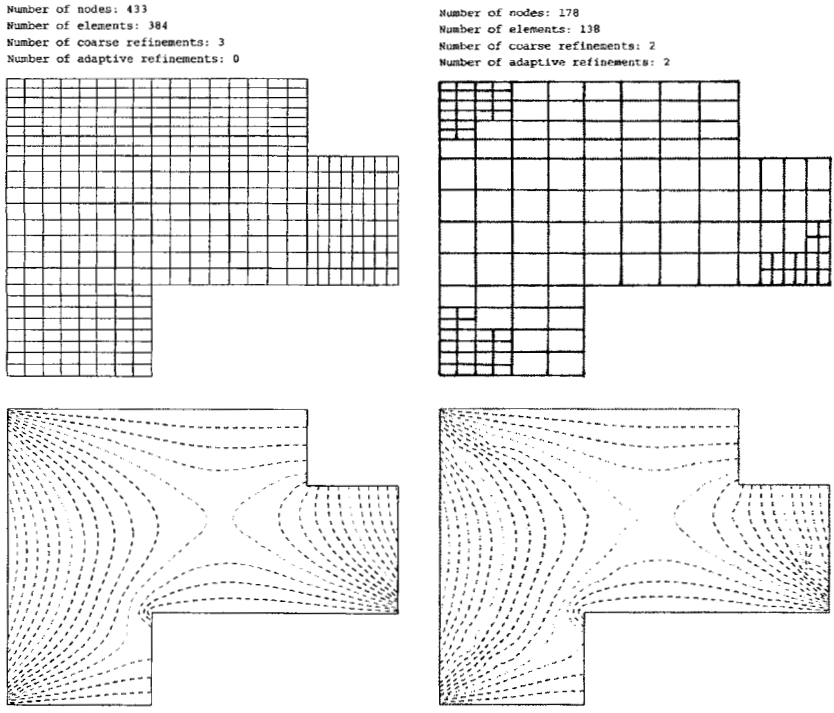

(a) (b)

Figure 8: FEM solutions (a) fine mesh and (b) adapted mesh [6].

Table 3. Comparison of results for problem 3 from FEM, BEM, and MFS

Method	mid-point (°C)	Elements	Nodes
FEM	75.899	384/138	433/178
BEM	75.885	36	37
MLM	75.893	0	96

7 Conclusions

An h-adapting, finite element method, a boundary element method, and a meshless method are used to calculate heat transfer in two-dimensions. All three techniques provide accurate results for the three example cases analyzed in this study. Each method has unique advantages along with some drawbacks. However, advances now being made in BEM and meshless methods will enable these two methods to eventually compete with the FEM on a much broader range of problems.

In the FEM model used in this study, an h-adapting technique was employed, along with mass lumping, Petrov-Galerkin weighting, and reduced integration to enhance overall speed. The use of local mesh refinement and

Paper from: *Advanced Computational Methods in Heat Transfer*, B Sunden and CA Brebbia (Editors).
ISBN 1-85312-906-2

unrefinement, coupled with Petrov-Galerkin weighting, produces very accurate results in regions where high activity occurs. Even with these enhancements, the BEM and MLM were clearly faster and required considerably less storage than the FEM, while providing nearly identical results to the FEM.

Details regarding the three models can be obtained by accessing the web site http://www.unlv.edu/Research_Centers/NCACM. Additional work is underway to develop a set of teaching models that will simulate 2-D incompressible fluid flow with convective heat transfer.

References

1. Lewis, R. W., Morgan, K., Thomas, H. R., & Seetharamu, K. N., *The Finite Element Method in Heat Transfer Analysis*, J. Wiley & Sons: Chichester, UK, 1996.
2. Huang, H-C., & Usmani, A. S., *Finite Element Analysis for Heat Transfer*, Springer-Verlag: London, UK, 1994.
3. Pepper, D. W., & Stephenson, D. E., An adaptive finite element model for calculating subsurface transport of contaminant, *Ground Water J.*, 33(3), pp. 486-496, 1995.
4. Heinrich, J. C., & Pepper, D. W., *Intermediate Finite Element Method: Fluid Flow and Heat Transfer Applications*, Taylor and Francis Pub. Co.: Philadelphia, PA., 1999.
5. Pepper, D. W., & Carrington, D. B., Benchmark Problems for Numerical Heat Transfer - Set 1: Laminar Convective Heat Transfer. *Int. Symp. Challenges & New Directions in Computation of Internal Flows*, Jan. 7-8, 2000, Madras, India.
6. Pepper, D. W., Carrington, D. B., and Gewali, L., A Web-based, Adaptive Finite Element Scheme for Heat Transfer and Fluid Flow. *ISHMT/ASME 4th Conf. on Heat and Mass Transfer*, Jan. 12-14, 2000, Pune, India.
7. Brebbia, C. A. & Dominguez, J., *Boundary Elements, An Introductory Course*, Comp. Mech. Pub., Southampton, U.K., 1989.
8. Wrobel, L. C. & DeFigueiredo, D. B., Chapter 5: Coupled Conduction-Convection Problems, in *Boundary Element Methods in Heat Transfer*, L. C. Wrobel and C. A. Brebbia (Eds.), Comput. Mech. Pub., Southampton, UK with Elsevier Appl. Sci., London, UK, pp. 123-144, 1992.
9. Lin, H. & Atluri, S. N., The meshless local Petrov-Galerkin (MLPG) method for solving incompressible Navier-Stokes Equation, *Computer Modeling in Eng. & Sci.*, 2, pp. 117-142, 2001.
10. Kansa, E. J., Multiquadric – A scattered data approximation scheme with applications to computational fluid dynamics II, *Computers Math. Appl.*, Vol. 19, No. 8/9, pp. 147-161, 1990.
11. Powell, M. J. D., The theory of radial basis function approximation in 1990, in *Advances in Numerical Analysis*, Vol. II, W. Light (Ed.), Oxford Sci.. Pub., Oxford, UK, pp. 105-210, 1992.
12. Incropera, F. P., & DeWitt, D. P., *Fundamentals of Heat and Mass Transfer*, 4th Ed., J. Wiley & Sons: New York, 1996.